Electronic Supplementary Information for

Enhancing the energy barrier and hysteresis temperature in two benchtop-stable Ho(III) single-ion magnets

Kexin Jia, Xixi Meng, Mengmeng Wang, Xiaoshuang Gou, Yu-xia Wang, Na Xu,* Wei Shi and Peng Cheng*

Department of Chemistry, College of Chemistry, Nankai University, Tianjin 300071, China.

E-mail: naxu@nankai.edu.cn; pcheng@nankai.edu.cn.

Table of Contents

1. Syntheses and physical measurements

General procedure for the synthesis of $[Ho(tprpo)_2(H_2O)_5]X_3 \cdot H_2O$

The solutions of $HoX_3 \cdot 6H_2O$ (X = Cl, **1**; Br, **2**) (0.05 mmol) in 0.5 mL methanol and tprpo (0.1 mmol) in 5 mL acetonitrile were mixed. The reaction mixture was sealed in a 10 mL vial and kept at 80 ºC for 12 h. After filtering, the clear filtrate was evaporated in an ambient environment, giving transparent microcrystals within two days. These microcrystals were further purified by washing with ethyl acetate and recrystallizing in acetonitrile to obtain hexagonal block crystals for single-crystal X-ray analysis.

$[Ho(tprpo)_2(H_2O)_5]Cl_3 \cdot H_2O$ (**1**) 22% yield based on $HoCl_3 \cdot 6H_2O$. Elemental analysis for $C_{24}H_{60}Cl_3N_6O_8P_2Ho$: calcd (%) C, 32.24; H, 6.76; N, 9.34; found (%) C, 31.91; H, 6.85; N, 8.96. FT-IR (cm^{-1}): 3228 (m), 3135 (m), 2958 (m), 2861 (m), 2283 (vw), 1659 (w), 1481 (w), 1446 (w), 1348 (w), 1291 (w), 1245 (m), 1204 (m), 1123 (s), 1072 (vs), 1008 (s), 962 (vw), 914 (w), 870 (m), 766 (m), 696 (s), 626 (m), 575 (vs), 529 (s).

$[Ho(tprpo)_2(H_2O)_5]Br_3 \cdot H_2O$ (**2**) 26% yield based on $HoBr_3 \cdot 6H_2O$. Elemental analysis for $C_{24}H_{60}Br_3N_6O_8P_2Ho$: calcd (%) C, 29.06; H, 5.89; N, 8.18; found (%) C, 29.16; H, 5.49; N, 8.37. FT-IR (cm^{-1}): 3334 (m), 3250 (m), 3176 (m), 2964 (m), 2863 (m), 2304 (vw), 1649 (w), 1636 (w), 1589 (vw), 1446 (w), 1344 (w), 1290 (w), 1243 (m), 1202 (m), 1110 (s), 1082 (vs), 1013 (s), 962 (m), 907 (m), 865 (m), 766 (m), 648 (s), 579 (vs), 537 (s).

Physical measurements

All chemicals and solvents were used in experiments as received without further treatment. The elemental analyses for carbon, hydrogen, and nitrogen were carried out using a PerkinElmer 240 CHN elemental analyzer. Powder X-ray diffraction patterns were recorded on a Rigaku Smartlab SE X-ray diffractometer. The Fourier Transform infrared spectroscopy (FTIR) measurements were carried out using a Bruker ALPHA FTIR spectrometer. Thermogravimetric analyses were performed on Mettler Toledo TGA 2 apparatus in the range of 40-800 ºC with a heating rate of 10 K min^{-1} under the nitrogen condition. The magnetic characterizations were performed on a Quantum Design SQUID MPMS VSM magnetometer. To eliminate the influence of diamagnetic atoms and sample holders, magnetic susceptibility data were corrected by Pascal's coefficient.

X-ray crystallography

The crystallographic data of **1** and **2** were measured on a Rigaku XtaLAB Mini II single-crystal diffractometer at room temperature with graphite monochromatic (Mo Kα X-ray source, λ = 0.71073 Å). The structures were solved by direct methods and further refined using the least-squares method with the *SHELXL-2017* programs. The non-hydrogen atoms have been refined using anisotropy thermal factors, while the hydrogen atoms were assumed to be isotropic and situated in theoretical positions.[1]

2. Structure and crystal data

Table S1. Comparison of the magnetic properties of **1** and **2** with reported Ho(III)-SIMs.

Complex	Symmetry	U_{eff} (K)	H_{dc} (Oe)	T_B (K)	Field sweep rate (Oe s^{-1})	Reference
$[Ho(tprpo)_2(H_2O)_5]Cl_3·H_2O$	D_{5h}	351	0	8	20	This work
$[Ho(tprpo)_2(H_2O)_5]Br_3·H_2O$	D_{5h}	418	0	15	20	This work
$[HoNi_5(quinha)_5F_2(dfpy)_{10}](ClO_4)·2EtOH$	D_{5h}	831	0	3.5	3200	2
$[Ho(OSiMe_3)_2(py)_5][BPh_4]$	D_{5h}	715	0	-	-	3
$[Ho(OCH(CH_3)C_6H_5)_2(py)_5][BPh_4]$	D_{5h}	499	0	-	-	3
$[Ho(OC_6H_3(CH_3)_2)_2(py)_5][BPh_4]$	D_{5h}	397	0	-	-	3
$[(L^1)_2Ho(H_2O)_5][I_3]·(L^1)_2·(H_2O)$	D_{5h}	355	0	4	270	4
$[Ho(CyPh_2PO)_2(H_2O)_5]I_3·2(CyPh_2PO)·H_2O·EtOH$	D_{5h}	341	0	3	1400	5
$[Ho(HMPA)_2(H_2O)_5]Br_3·2HMPA$	D_{5h}	320	0	-	-	6
$[Ho(HMPA)_2(H_2O)_5]_2Cl_6·2HMPA·2H_2O$	D_{5h}	290	0	-	-	6
$HoSc_2N@C_{80}$	C_∞	16.5	2000	-	-	7
[(Cp*)Ho(COT)]	C_∞	7.4, 3.6	0	-	-	8
$[(Cp^*)Ho_{0.05}Y_{0.95}(COT)]$	C_∞	33.8, 24.4	0	-	-	8
$[Ho_4(\mu_3\text{-}OH)_2(L^2)_4(piv)_2(DMF)_2]·2DMF$	D_{4d}	21.5	5000	-	-	9
$[Pc_2Ho_{0.02}Y_{0.98}][TBA]$	D_{4d}	-[a]	-	0.5	2800	10
$Ho(CH_2SiMe_3)_3(THF)_2$	C_s	76	0	-	-	11
$[(L^3)_2Co_2Ho][NO_3]$	I_h	8	0	-	-	12
$K_{12}[HoP_5W_{30}O_{110}]·nH_2O$	-	0.8	0	2	90	13
$Ho(CH_2SiMe_3)_3(QN)_2$	C_s	-[b]	0	-	-	11
$Ho(CH_2SiMe_3)_3(OPCy_3)_2$	C_s	-[b]	0	-	-	11
$Ho(CH_2SiMe_3)_3(Lut)_3$	O_h	-[b]	0	-	-	11
$Na_9[Ho(W_5O_{18})_2]$	D_{4d}	-[b]	0	-	-	14
$K_{13}[Ho(\beta_2\text{-}SiW_{11}O_{39})_2]$	D_{4d}	-[b]	0	-	-	14
$[Ho(\beta\text{-}Mo_8O_{26})_2]^{5-}$	D_{4d}	-[b]	0	-	-	15
$[Ho(bphosCN)_3(H_2O)]·8H_2O$	C_{2v}	-[b]	0	-	-	16

[a]The data of ac susceptibility was not mentioned. [b]Ac magnetic susceptibilities showed frequency-dependent signals but no clear peak under zero dc field. tprpo = trispyrrolidinophosphineoxide; H_2quinha = quinaldichydroxamic acid; dfpy = 3,5-difluoropyridine; py = pyridine; L^1 = ^{t}BuPO(NH^{i}Pr)$_2$; HMPA = hexamethylphosphorictriamide; Cp* = pentamethylcyclopentadienide; COT = cyclooctatetraene; H_2L^2 = 2-hydroxy-3-methoxy-phenylsalicylaldimine; piv = pivalate; TBA = tetrabutylammonium; Pc = phthalocyanine; H_3L^3 = (*S*)P[N(Me)NdCH-C_6H_3-2-OH-3-OMe]$_3$; QN = quinuclidine; Lut = 3,5-lutidine; bphosCN = cyanomethylene-bis(5,5-dimethyl-2-oxo-1,3,2-λ^5-dioxa-phosphorinane.

Table S2. Crystal data and structure refinements of **1** and **2**.

Compound	**1**	**2**
CCDC	2059754	2059755
Formula	$C_{24}H_{60}Cl_3N_6O_8P_2Ho$	$C_{24}H_{60}Br_3N_6O_8P_2Ho$
Formula weight	894.00	1027.38
T (K)	293(2)	293(2)
Crystal System	orthorhombic	orthorhombic
Space Group	*Pbca*	*Pbca*
a (Å)	9.9663(3)	10.0871(3)
b (Å)	26.9370(9)	26.8701(7)
c (Å)	30.2924(9)	30.9089(12)
α (deg)	90	90
β (deg)	90	90
γ (deg)	90	90
Z	8	8
V (Å^3)	8132.4(4)	8377.6(4)
ρ_{calc} (g/cm^3)	1.460	1.629
μ (mm^{-1})	2.267	4.871
R_{int}	0.0609	0.0495
GOF	1.038	1.017
R_1,wR_2 [$I > 2\sigma(I)$][a]	0.0546, 0.1327	0.0416, 0.0816
R_1,wR_2 (all data)[b]	0.0833, 0.1461	0.0822, 0.0929

$_aR_1 = \sum(|F_o| - |F_c|)/\sum|F_o|$. $_bwR_2 = \left[\sum w\left(F_o^2 - F_c^2\right)^2/\sum w\left(F_o^2\right)^2\right]^{1/2}$.

Table S3. Selected bond lengths and angles of **1**.

Bond/Angles	°/Å	Bond/Angles	°/Å
Ho-O1	2.205(5)	O2-Ho1-O6	87.52(2)
Ho-O2	2.215(5)	O3-Ho1-O6	143.90(2)
Ho-O3	2.366(5)	O4-Ho1-O6	144.36(2)
Ho-O4	2.344(5)	O1-Ho1-O5	90.10(2)
Ho-O5	2.343(5)	O2-Ho1-O5	87.91(2)
Ho-O6	2.356(5)	O3-Ho1-O5	144.14(2)
Ho-O7	2.355(5)	O4-Ho1-O5	72.52(2)
O1-Ho1-O2	177.94(19)	O6-Ho1-O5	71.96(2)
O1-Ho1-O3	90.65(2)	O1-Ho1-O7	89.47(2)
O2-Ho1-O3	91.28(2)	O2-Ho1-O7	91.82(2)
O1-Ho1-O4	90.16(2)	O3-Ho1-O7	71.79(2)
O2-Ho1-O4	89.76(2)	O4-Ho1-O7	143.43(19)
O3-Ho1-O4	71.65(2)	O6-Ho1-O7	72.20(2)
O1-Ho1-O6	91.35(2)	O5-Ho1-O7	143.98(2)
Ho···Cl1	4.6160(2)	Ho···Cl3	4.6922(2)
Ho···Cl2	4.5977(2)		

Table S4. Selected bond lengths and angles of **2**.

Bond/Angles	°/Å	Bond/Angles	°/Å
Ho-O1	2.193(4)	O2-Ho1-O6	90.83(15)
Ho-O2	2.198(4)	O3-Ho1-O6	142.86(17)
Ho-O3	2.336(5)	O4-Ho1-O6	144.37(14)
Ho-O4	2.348(4)	O1-Ho1-O5	92.66(14)
Ho-O5	2.353(4)	O2-Ho1-O5	87.10(14)
Ho-O6	2.354(4)	O3-Ho1-O5	144.85(17)
Ho-O7	2.372(4)	O4-Ho1-O5	72.26(14)
O1-Ho1-O2	178.80(15)	O6-Ho1-O5	72.20(14)
O1-Ho1-O3	90.12(17)	O1-Ho1-O7	89.38(14)
O2-Ho1-O3	89.41(17)	O2-Ho1-O7	91.51(15)
O1-Ho1-O4	88.92(14)	O3-Ho1-O7	71.06(17)
O2-Ho1-O4	89.89(15)	O4-Ho1-O7	143.77(14)
O3-Ho1-O4	72.77(17)	O6-Ho1-O7	71.81(14)
O1-Ho1-O6	90.21(15)	O5-Ho1-O7	143.96(14)
Ho···Br1	4.8452(9)	Ho···Br3	4.7671(1)
Ho···Br2	4.7883(9)		

Table S5. Continuous shape measures calculations for Ho^{III} ion in **1** and **2**.

Symmetry	Shape	Deviation for 1	Deviation for 2
D_{7h}	Heptagon	34.501	34.165
C_{6v}	Hexagonal pyramid	25.663	25.323
D_{5h}	Pentagonal bipyramid	0.112	0.132
C_{3v}	Capped octahedron	8.061	8.125
C_{2v}	Capped trigonalprism	6.203	6.228
D_{5h}	Johnson pentagonal bipyramid	2.694	2.595
C_{3v}	Johnson elongated triangularpyramid	24.549	24.152

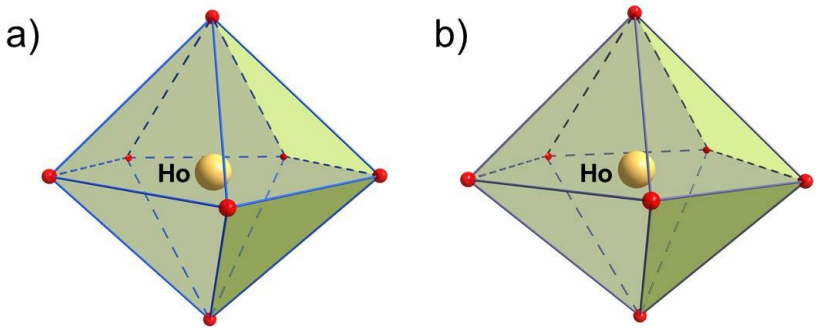

Figure S1. Coordination environment of Ho^{III} ion of **1** (a) and **2** (b).

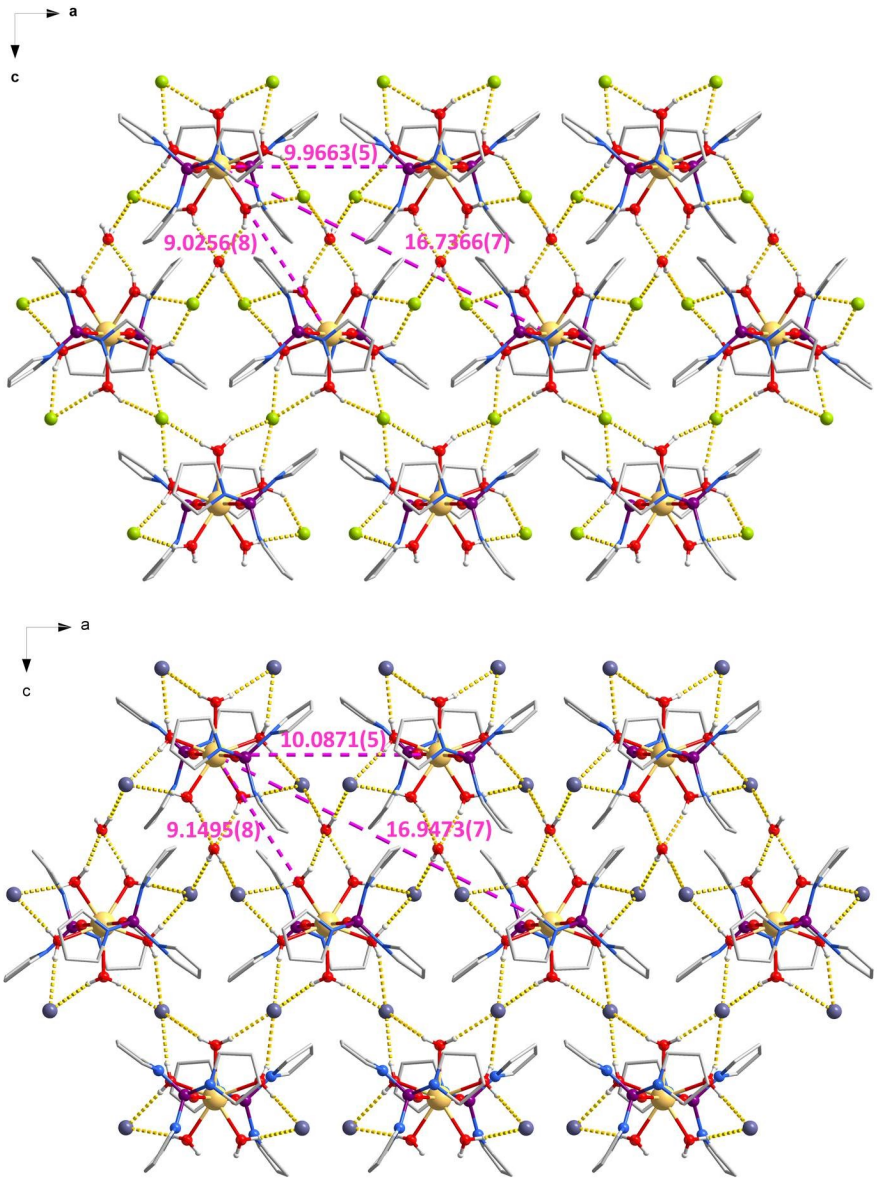

Figure S2. Crystal structures of **1** (up) and **2** (down) viewed along the *b* axis. Hydrogen atoms of tprpo are omitted for clarity. Atom color codes: Ho, yellow; O, red; N, light blue; P, violet; C, gray; H, light gray; Cl, lime; Br, blue gray. Gold dashed lines represent the hydrogen bonds between coordinated water molecules and free water molecules and counter ions. The pink dash lines correspond to the distances between neighboring Ho^{III} centers.

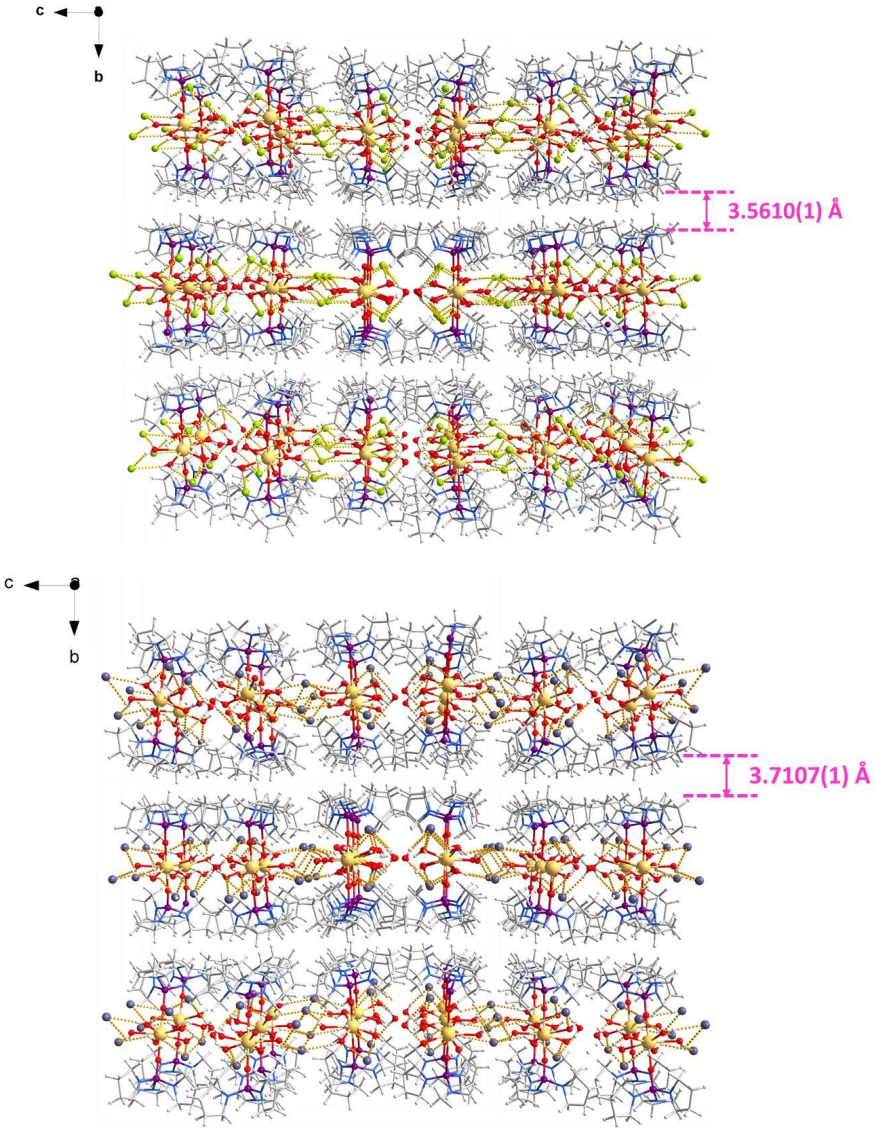

Figure S3. The 3D packing structure of **1** (up) and **2** (down). Atom color codes: Ho, yellow; O, red; N, light blue; P, violet; C, gray; H, light gray; Cl, lime; Br, blue gray. Gold dashed lines represent the hydrogen bonds between coordinated water molecules and free water molecules and counter ions.

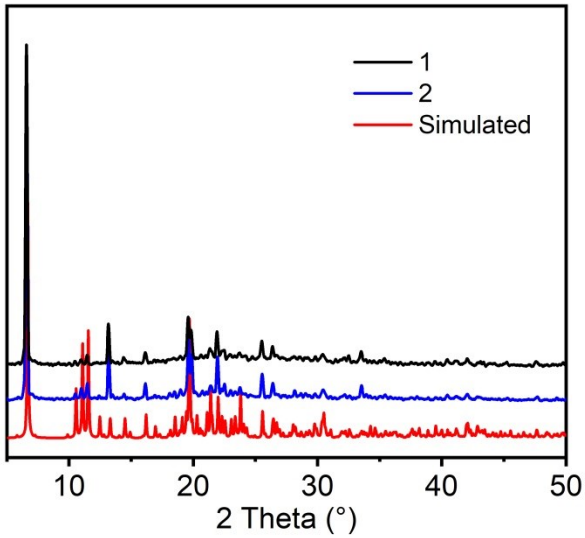

Figure S4. The powder X-ray diffraction patterns of **1** and **2** compared with the simulated pattern from the single-crystal data of **1**.

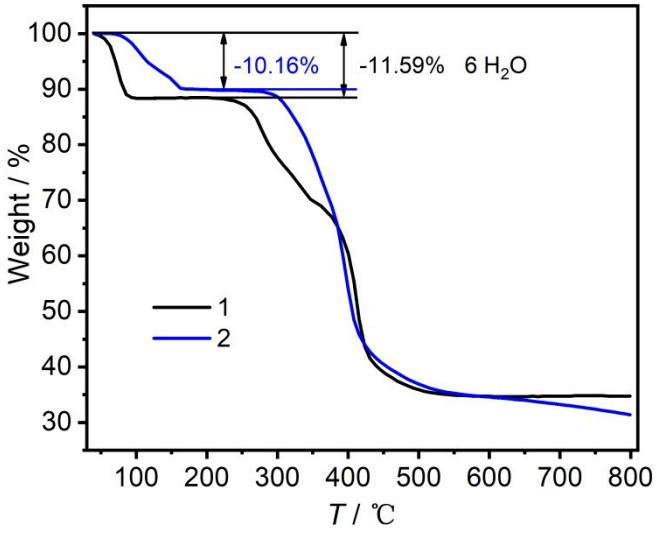

Figure S5. TGA of **1** and **2**.

3. Magnetic characterization data

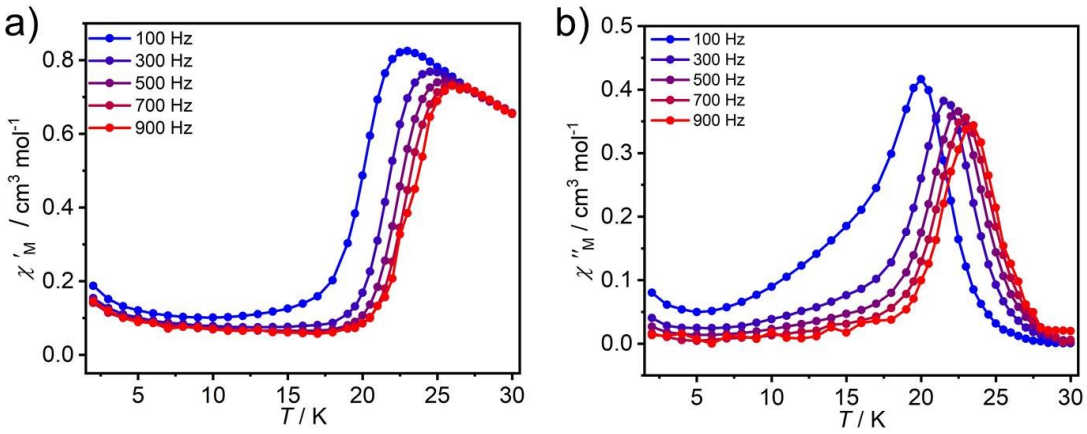

Figure S6. Frequency-dependent of in-phase and out-of-phase ac magnetic susceptibilities of **1** under zero dc field.

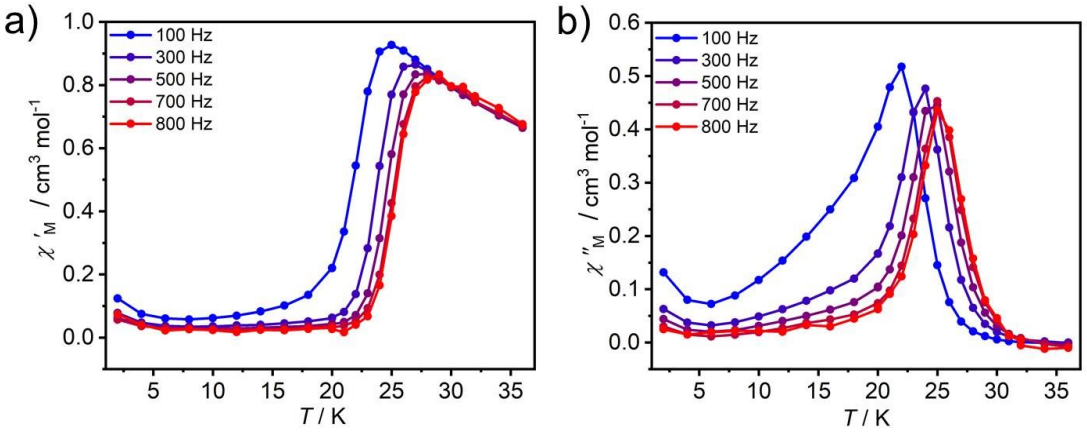

Figure S7. Frequency-dependent of in-phase and out-of-phase ac magnetic susceptibilities of **2** under zero dc field.

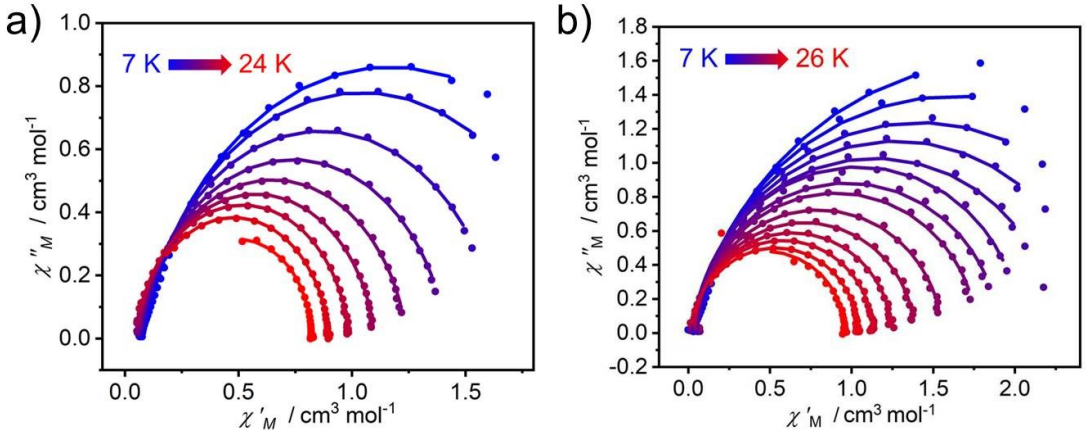

Figure S8. The Cole-Cole plots for **1** (a) and **2** (b). Solid lines are the fits with the Debye models.

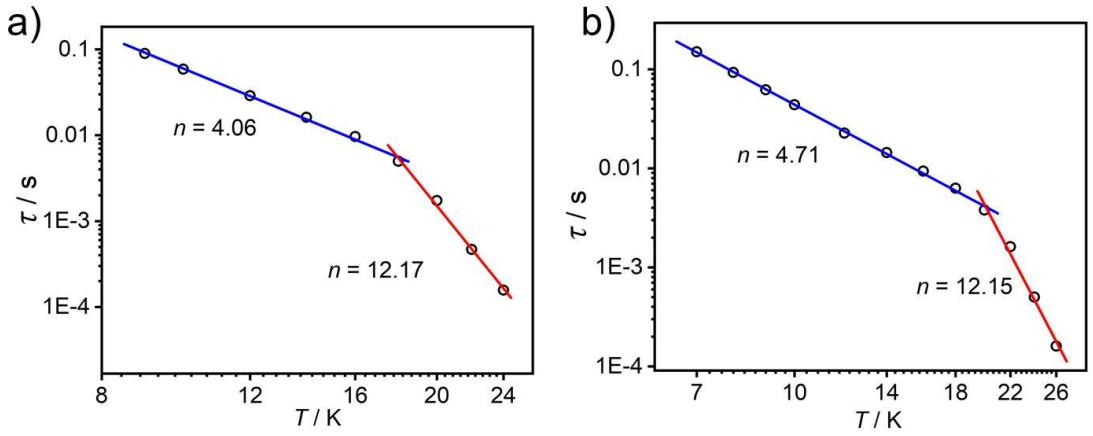

Figure S9. The τ *vs.* T^{-n} plots shown in log-log scale for **1** (a) and **2** (b).

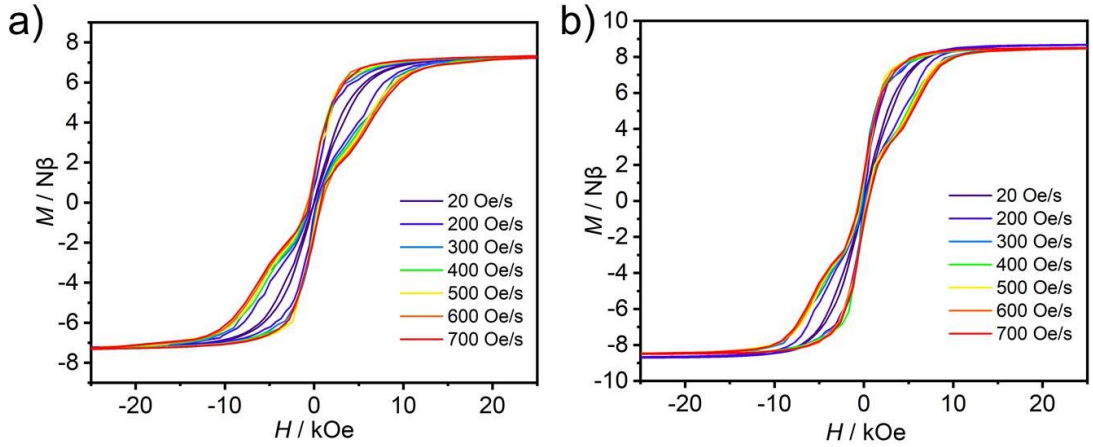

Figure S10. Magnetic hysteresis loops of **1** (a) and **2** (b) at 2 K and different field sweep rates.

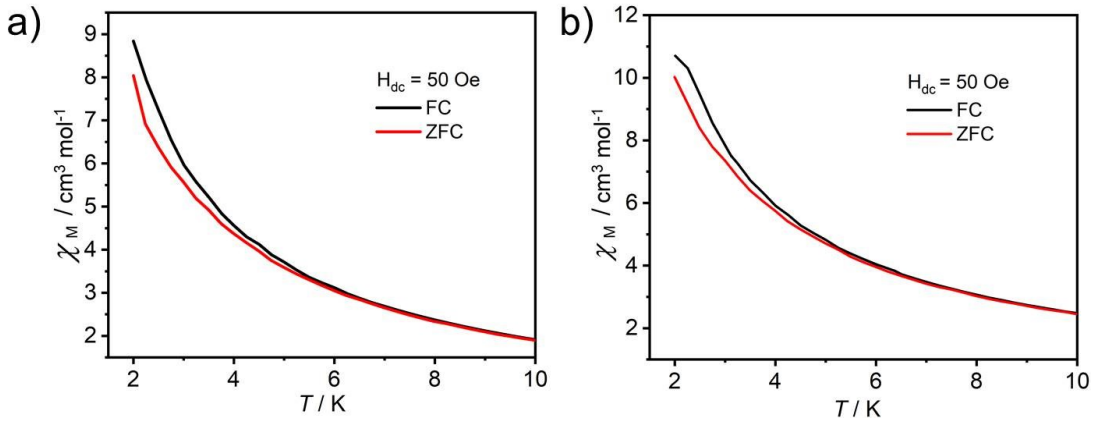

Figure S11. The Field cooled (FC) and Zero-Field cooled (ZFC) magnetic susceptibility of **1** (a) and **2** (b).

Table S6. The best fitting parameters of Cole-Cole plots of **1** under zero dc field.

T (K)	χ_s (cm^3 mol^{-1})	χ_t (cm^3 mol^{-1})	τ (s)	α
7	0.08944	3.23955	0.27758	0.20183
8	0.08598	2.63315	0.14865	0.16767
9	0.08139	2.25678	0.08957	0.14719
10	0.07647	2.01193	0.05897	0.13624
12	0.06901	1.65638	0.02884	0.11873
14	0.06231	1.41948	0.01621	0.11331
16	0.05818	1.24141	0.00964	0.10172
18	0.05261	1.10094	0.00498	0.08468
20	0.0508	0.9868	0.00174	0.06295
22	0.05936	0.89783	4.6727E-4	0.05538
24	0.18493	0.82201	1.57029E-4	0.00999

Table S7. The best fitting parameters of Cole-Cole plots of **2** under zero dc field.

T (K)	χ_s (cm^3 mol^{-1})	χ_t (cm^3 mol^{-1})	τ (s)	α
7	0.04321	3.87826	0.14994	0.11384
8	0.04515	3.21341	0.09275	0.08178
9	0.04222	2.7872	0.062	0.06595
10	0.04369	2.50228	0.04377	0.05445
11	0.02667	2.26238	0.03164	0.05362
12	0.05594	2.02959	0.02262	0.00682
13	0.03768	1.9045	0.01832	0.03629
14	0.04045	1.76894	0.01443	0.03086
16	0.03771	1.55352	0.00938	0.02855
18	0.03528	1.38573	0.00628	0.0242
20	0.02794	1.24587	0.00379	0.02032
22	0.02767	1.13	0.00162	0.00714
24	0.03546	1.0374	5.00388E-4	2.11812E-15
26	2.99731E-15	0.95761	1.60026E-4	7.01192E-15

References

1 V. Dolomanov, L. J. Bourhis, R. J. Gildea, J. A. K. Howard and H. Puschmann, *J. Appl. Cryst.*, 2009, **42**, 339.

2 S.-G. Wu, Z.-Y. Ruan, G.-Z. Huang, J.-Y. Zheng, V. Vieru, G. Taran, J. Wang, Y.-C. Chen, J.-L. Liu, L. T. A. Ho, Liviu F. Chibotaru, W. Wernsdorfer, X.-M. Chen and M.-L. Tong, *Chem*, 10.1016/j.chempr.2020.12.022.

3 Y. Ma, Y.-Q Zhai, Y.-S. Ding, T. Han and Y.-Z. Zheng, *Chem. Commun.*, 2020, **56**, 3979.

4 S. K. Gupta, T. Rajeshkumar, G. Rajaraman and R. Murugavel, *Dalton Trans.*, 2018, **47**, 357.

5 Y.-C. Chen, J.-L. Liu, W. Wernsdorfer, D. Liu, L. F. Chibotaru, X. M. Chen and M.-L. Tong, *Angew. Chem. Int. Ed.*, 2017, **56**, 4996.

6 L.-L. Li, H.-D. Su, S. Liu and W.-Z. Wang, *Dalton Trans.*, 2020, **49**, 6703.

7 J. Dreiser, R. Westerström, Y. Zhang, A. A. Popov, L. Dunsch, K. Krämer, S.-X. Liu, S. Decurtins and T. Greber, *Chem. Eur. J.*, 2014, **20**, 13536.

8 S.-D. Jiang, S.-S. Liu, L.-N. Zhou, B.-W. Wang, Z.-M. Wang and S. Gao, *Inorg. Chem.*, 2012, **51**, 3079.

9 W.-W. Kuang, L.-L. Zhu, Y. Xu and P.-P. Yang, *Inorg. Chem. Commun.*, 2015, **61**, 169.

10 N. Ishikawa, M. Sugita and W. Wernsdorfer, *J. Am. Chem. Soc.*, 2005, **127**, 3650.

11 S.-M. Chen, Y.-Q. Zhang, J. Xiong, B.-W. Wang and S. Gao, *Inorg. Chem.*, 2020, **59**, 5835.

12 V. Chandrasekhar, B. M. Pandian, J. J. Vittal and Rodolphe Clérac, *Inorg. Chem.*, 2009, **48**, 1148.

13 S. C.-Serra, J. M. C.-Juan, E. Coronado, A. G.-Arino, A. Camon, M. Evangelisti, F. Luis, M. J. M.-Pérez and J. Sesé, *J. Am. Chem. Soc.*, 2012, **134**, 14982.

14 M. A. AlDamen, S. C.-Serra, J. M. C.-Juan, E. Coronado, A. G.-Ariño, C. M.-Gastaldo, F. Luis and O. Montero, *Inorg. Chem.*, 2009, **48**, 3467.

15 J. J. Baldoví, Y. Duan, C. Bustos, S. C.-Serra, P. Gouzerh, R. Villanneau, G. Gontard, J. M. C.-Juan, A. G.-Ariño, C. G.-Saiz, *Dalton Trans.*, 2016, **45**, 16653.

16 C. Maxim, D. G. Branzea, C. Tiseanu, M. Rouzieres, R. Clerac, M. Andruh and N. Avarvari, *Inorg. Chem.*, 2014, **53**, 2708.